Springer

KSME

Journal of Mechanical Science and Technology 30 (4) (2016) 1507~1525
www.springerlink.com/content/1738-494x(Print)/1976-3824(Online)
DOI 10.1007/s12206-016-0304-5

Investigation of in-train stability and safety assessment for railway vehicles during braking †

Lai Wei*, Jing Zeng and Qunsheng Wang

State Key Laboratory of Traction Power, Southwest Jiaotong University, Chengdu, China

(Manuscript Received July 3, 2015; Revised December 5, 2015; Accepted December 12, 2015)

Abstract

In-train stability of railway vehicles has becoming a major concern for railway vehicles, which refers to the jackknifing behavior of couplers under large in-train forces. For the train to train rescue scenario, braking induced impacts from couplers can adversely affect the dynamic performance of the coupled train. It is indicated from field tests that in-train forces if combined with large rotational angles of couplers can produce vertical components, which will further lead to the interference of adjacent carbodies and structural damages. In this paper, the dynamic model of the train and coupler system is developed. The model verifications are conducted by comparing the calculated responses with the tested results. The safety indices are formulated on the basis of which the running safety of the coupled train is evaluated. The propelling test in the laboratory is conducted to reproduce the coupler jackknifing behavior. The quasi-static analysis and anti-jackknifing mechanism under compressing in-train forces are analysed. Parametric studies are then conducted to propose some limitations for the application of train to train rescue. It is indicated from numerical and testing results that the decrease of the braking deceleration or a limitation of the free rotational angle of couplers is beneficial to lower the amplitude of braking induced impacts.

Keywords: In-train stability; Train to train rescue; Braking; Coupler jackknifing; Dynamic model; Test verification; Safety analysis; Force states; Laboratory experiments; Braking deceleration; Coupler free rotational angle

1. Introduction

Once a train is disabled in a high speed railway line, an assisting locomotive is traditionally used to rescue the disabled train. In order to increase the efficiency of train rescue and restore line operating orders quickly, train to train rescue is commonly used nowadays. Then the emergency couplers are specially designed to make the mechanical connections between different types of couplers possible [1]. However, as the disabled train is out of the ability of braking, the application of braking forces by the assisting train will generate longitudinal in-train forces and may lead to the so called "coupler jackknifing" behaviour. Jackknifing means the folding of an articulated vehicle or coupler, such that it resembles the acute angle of a folding pocket knife. If two vehicles are connected with a pair of couplers, the trailer vehicle can push from behind until spinning around or limited by boundaries. In fact, the rotations of the coupler with respect to the lateral or vertical pins are free. Thus, the coupler jack-knifing behavior reflects the relative motions between adjacent carbodies. This may be caused by equipment failure, improper braking, or adverse track excitations. In consequence, the lateral or vertical force components of in-train forces may affect the running safeties of the coupled train [2].

In the field of heavy haul trains and locomotives, derailment accidents due to coupler jackknifing under buff forces were also reported in literatures. In recent years, the Transportation Safety Board of Canada (TSB) has investigated a number of rail accidents, in which coupler jackknifing under longitudinal in-train buff forces was a contributing factor [3]. In the Association of American Railways (AAR), studies of the in-train stability for freight cars date back to 1955 [4]. A prototype buff and draft car was designed, constructed and tested so as to determine the maximum lateral load that can be applied safely. In order to analyse the coupler angle on curved tracks, the Coupler Angling Behavior Software was also developed [5]. McClanachan et al. [6, 7] pointed out that longitudinal train dynamics can be divided into longitudinal-rotational, -lateral and -vertical dynamics. The combination of in-train forces and coupler angles produce lateral or vertical force components, which could lead to the increase of derailment coefficient and wheel unloading ratio. Cole et al. [8] took the coupling-free slack and nonlinear characteristics of buffer into consideration to study the coupler jackknifing and string-lining problem. It is also known that lateral force components and impacts from couplers can adversely affect wagon stabil-

*Corresponding author. Tel.: +86 15902839082, Fax.: +86 87600868
E-mail address: 707101305@qq.com
† Recommended by Associate Editor Eung-Soo Shin

ity [9]. It was reported that the coupler lateral-rotational behavior contributed a lot to gauge widening and rail rollover derailments under braking forces [10, 11]. Luo and colleagues [12, 13] have focused a lot on the investigation of coupler stability mechanism and the dynamic modeling of different types of couplers.

As the in-train stability of vehicles is of importance to the safe operation, some standards or technique specifications have been formulated. For a new vehicle design in AAR, it is recommended that an analysis should be made for a 250000-pound sustained buff and draft load, on a 10-degree curve or tighter, and a coupling arrangement with at least one additional vehicle which provides the longest possible truck base and overhang [14]. In Australia, the standard AS7509.2 [15] describes the method to evaluate whether the lateral component of longitudinal train forces in curves will be sufficient to cause wheel lift on rolling stock and subsequent derailment. During the in-train stability test on curved tracks, any wheel lift or flange climb lifting the centre of the tread off the rail head by more than 10 mm constitutes failure. In Europe, it is also recognized that longitudinal forces within trains have the potential to increase the risk of derailment when negotiating curves [16]. For conventional trains this risk is regarded as low. In the case of freight vehicles the procedure defined in UIC 530-2 shall be used. The permissible longitudinal compressive forces are determined by carrying out propelling tests on a S-shaped curve with the radius of 150 m [17].

In general, most of the current works are focused on studying the longitudinal dynamics of freight cars or locomotives on curved tracks. However, the coupler vertical jackknifing behavior and operating safety assessment for the train to train rescues, especially for high speed trains, is more significant. In this paper, the coupler vertical angling behavior occurring in the field test of train to train rescue is introduced. The in-train forces are generated due to the application of braking by the assisting train. The longitudinal forces if combined with coupler rotational angles can produce vertical force components which affects the running safeties of the coupled trains. The dynamic models of typical train to train rescue scenarios are developed by using the simulation package SIMPACK. The calculated responses, e.g. the in-train forces, vehicle decelerations, wheel unloading ratio, pitch angles, etc., are also verified by field test results. The safety analyses for train to train rescue scenarios are then carried out. The propelling test in the laboratory is conducted for two coupled couplers to reproduce the coupler jackknifing behavior. The quasi-static geometry and force analyses and anti-jackknifing mechanism under compressing in-train forces are conducted. The influences of some basic parameters on the coupler jackknifing are studied. Parametric studies are then conducted to propose some limitations for the application of train to train rescues.

The objective of this paper is to introduce the so called in-train stability problem, a new phenomenon under the braking condition. The investigations are conducted by the field test, numerical simulations as well as laboratory experiments so as to give insight into its mechanism and consequent effects. Some measures or recipes are discussed to prevent the potential development of the jackknifing from both the quasi-static equations and dynamic computations.

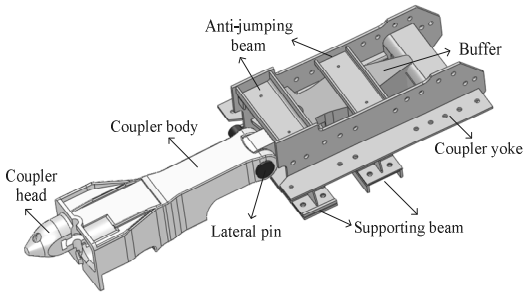

(a) Shibata coupler

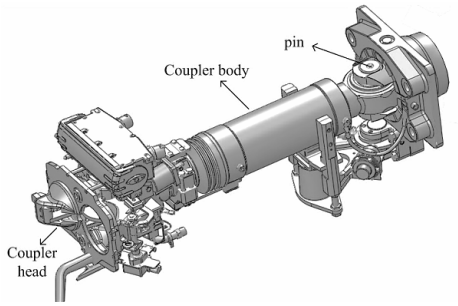

(b) Type 10 coupler

Fig. 1. Typical coupler structures.

2. Coupler angling behavior in field test of train to train rescue scenario

There exist different forms of coupler systems in the railway vehicles, which vary in mechanical structures, working mechanisms and buffer characteristics, etc. In the field of high speed trains, the Shibata coupler used for Shinkansen vehicles and the Type10 coupler for ICE, TGV and AVE vehicles are two of the most representative ones. Japanese Railway (JR) has widely standardized on the Shibata coupler, initially developed by a Railway engineer, Mamoru Shibata in the 1930's. Fig. 1(a) shows the mechanical illustration of the Shibata coupler, included by the coupler body, coupler yoke, circular pins and some accessory components. The part with free rotations about the pins is called coupler body, while the whole section between the pins and the carbody is called yoke. The circular pins allow the coupler body's free rotations relative to the yoke when negotiating horizontal or vertical curves. The yoke is supported by beams and limited by two anti-jumping beams. Relative movements or rotations are allowable due to the slacks and elasticity of these beams. Besides, the Scharfenberg coupler is a commonly used type of fully automatic railway coupling, which is designed in 1903 by Karl Scharfenberg in Königsberg, Germany. This coupler is superior in many ways to other couplers because it makes the electrical and the

Table 1. List of test instrumentations of one vehicle.

No.	Type	Location	Direction
1	Instrumented couplers	Carbody end	X
2	Video	Coupler	/
3	Accelerometer 1	Carbody front	XYZ
4	Accelerometer 2	Carbody center	XYZ
5	Accelerometer 3	Carbody rear	XYZ
6	Dis transducer 1	Air spring front	Z
7	Dis transducer 2	Air spring rear	Z
8	Dis transducer 3	Primary spring front	Z
9	Dis transducer 4	Primary spring rear	Z
10	Dis transducer 5	Front coupler and carbody	Z
11	Dis transducer 6	Rear coupler and carbody	Z
12	Dis transducer 7	In-train displacement	Z

pneumatic connections automatic, see Fig. 1(b). The Type10 latch system automatic centre buffer coupler has been standardized in Europe, as noted in Ref. [18].

The line tests for the train to train rescue scenarios were conducted to validate the longitudinal dynamic performance. The illustrations of the coupled assisting and disabled train are shown in Fig. 2. The transducers and accelerometers are arranged to measure the braking induced impacts of the coupler and vehicle systems. Here, the disabled train means the train without the ability of applying braking. The instrumentations used in the field test are listed in Table 1 and its installation locations are illustrated in Fig. 2(c). The instrumented coupler was adopted to measure the generated in-train forces during braking. The video camera was installed to monitoring the coupler behavior during braking. The accelerometers were arranged on the carbody front, center and rear floor to obtain the braking induced impact. The displacement (shorted as 'dis') transducers were used to measure the relpative displacements of the suspension system, e.g. air spring and primary spring. The measured results can be used to calculate the carbody pitch angle. The dis transducers were also installed between the coupler and the coupler so as to calculate the relative pitch angle of the coupler. Moreover, the relative displacements between adjacent carbodies were also measured.

For case A, both the assisting and the disabled train were equipped with Shibata couplers. The coupled train was consisted of 8 assisting cars and 8 disabled cars. The applied emergency braking deceleration was 1.395 m/s^2 and the running speed for the coupled train was 60 km/h. The installing heights of couplers in the central section are both 1000 mm. For case B, the assisting train in the front was equipped with Shibata couplers, while the disabled train in the rear with Voith type 10 couplers. The coupled train was consisted of 16 assisting cars and 16 disabled cars. The emergency coupler was used to make mechanical connections possible between these two types of couplers in the central section. The braking

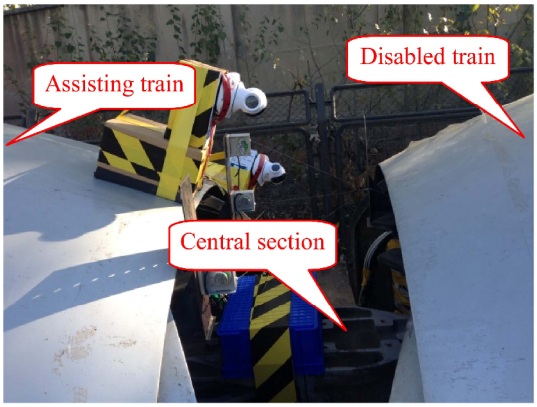

(a) Case A

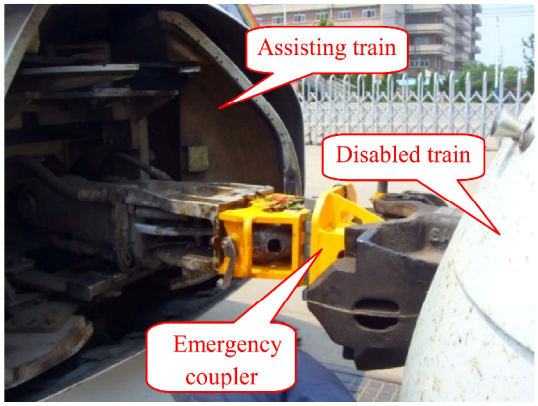

(b) Case B

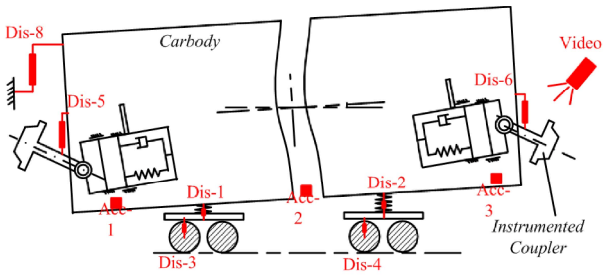

(c) Illustration of test instrumentations

Fig. 2. Illustration of train to train rescue scenarios in the field test.

forces can be only applied by the assisting train and the deceleration of the emergency braking is 1.395 m/s^2. The running speed for the coupled train was 20 km/h before the application of braking forces. In the central connection section, the installing height of the Shibata coupler is 120 mm higher than the type 10 coupler.

Compressing in-train forces under braking conditions have an adverse effect on the vertical and lateral stability of either the train or the coupler system. The pitch motion of the carbody generates a vertical relative displacement between adjacent vehicles, which leads to the geometry interference of in-train connections. The measured pitch angles of carbody and coupler for case A are shown in Fig. 3. The measured pitch

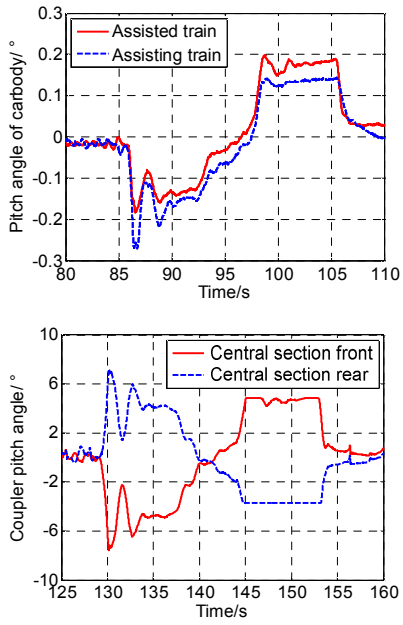

Fig. 3. Measured pitch angles of carbody and coupler for case A.

angle of the carbody is determined by the vertical displacements of the secondary suspensions. The angling behaviour of the coupler, if combined with longitudinal buff forces, can generate a force component. In consequence, one or several of the following conditions may happen on tangent track:

- Coupler vertical jackknifing;
- Carbody pitch motion;
- Wheel unloading.

The geometrical analyses of two coupled Shibata couplers for case B which is adjacent to the central section are shown in Fig. 4. It is indicated from the tested results that coupler jackknifing behaviour happed during the braking progress. The rotation of the coupler body with respect to the lateral pin is free. Normally, the coupler yoke is constrained by actual boundary conditions, e.g. the supporting beam and the anti-jumping beam. However, elastic and plastic deformation of the beams may happen due to the braking induced impacts. Therefore, the longitudinal, vertical movement and the pitch rotation of the coupler yoke are free in the scenario of large in-train forces. The compressing in-train forces if combined with the coupler vertical jackknifing can generate vertical force components on the front supporting beam. On the contrary, a reacting force is produced on the anti-jumping beam, from which the vertical force component is transferred to the accessary plate and the carbody underframe. The produced vertical force is the main indicator of causing structural damage to local components.

Besides, some of the following conditions may happen on curved track:

- Coupler lateral jackknifing;
- Carbody yaw motion;
- Risk of wheel climbing and even derailment.

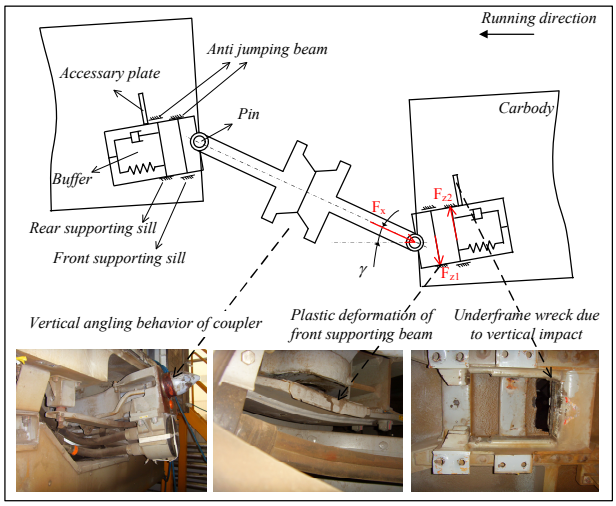

Fig. 4. Testing analysis of coupler jackknifing behaviour for case B.

Wheel climb and track gauge widening may occur in extreme conditions especially for locomotives and freight cars [10]. For high speed trains, the lateral rotation angle of the coupler in normal conditions is relatively small for the assisting train on tangent tracks or curved tracks with large radii. The relatively large yaw angle for the train operating on the small-radius curved track in the depot is not considered in this paper.

3. Dynamic simulations

3.1 Modeling

The dynamic simulations for the train to train rescue scenario will be conducted in this section. The dynamic models of the train and coupler system are developed using the simulation package SIMPACK, see Fig. 5. In this model, three assisting and three disabled vehicles close to the central connecting section are built with considering all the Degrees of freedom (DOF), while other vehicles are simplified as dummy vehicles with only longitudinal DOF, see Fig. 5(a).

The scheme of the vehicle multi-body system is shown in Fig. 5(b), from which It is seen from Fig. 5(a) that one car body is individually supported by two bogies, while one bogie is consisted of two conventional wheel sets. In the vehicle model, each car body or bogie frame has six independent DoFs which allows free movements or rotations with respect to the lateral, vertical and longitudinal direction, respectively. The vertical and roll motion of the wheel set are dependent on the lateral and yaw motion, so the wheel set has four independent and two dependent DoFs. The summary of the DOFs of the couplers is shown in Table 2.

The nonlinear characteristics of vehicle system and in-train interactions are considered and the train system dynamic equation can be expressed as below:

$$M\ddot{q} + C\dot{q} + Kq = f(\ddot{q},\dot{q},q,t) + De \tag{1}$$

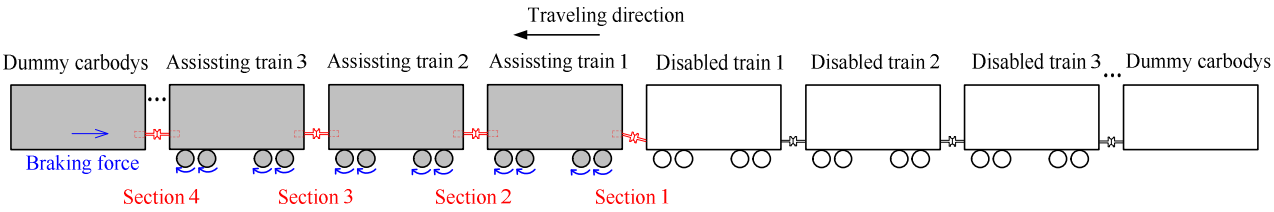

(a) Train configuration

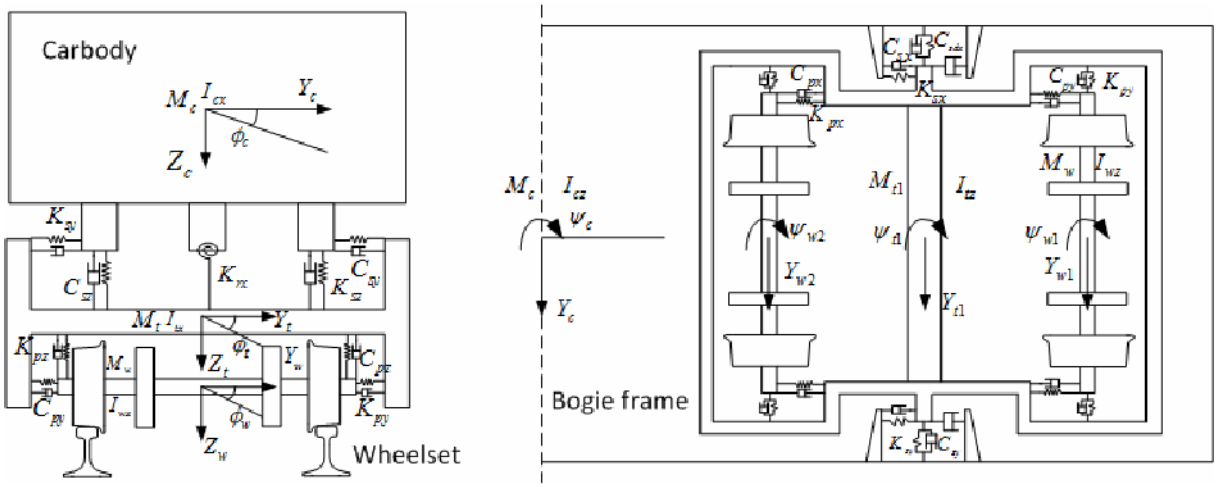

(b) Scheme of vehicle multi-body system

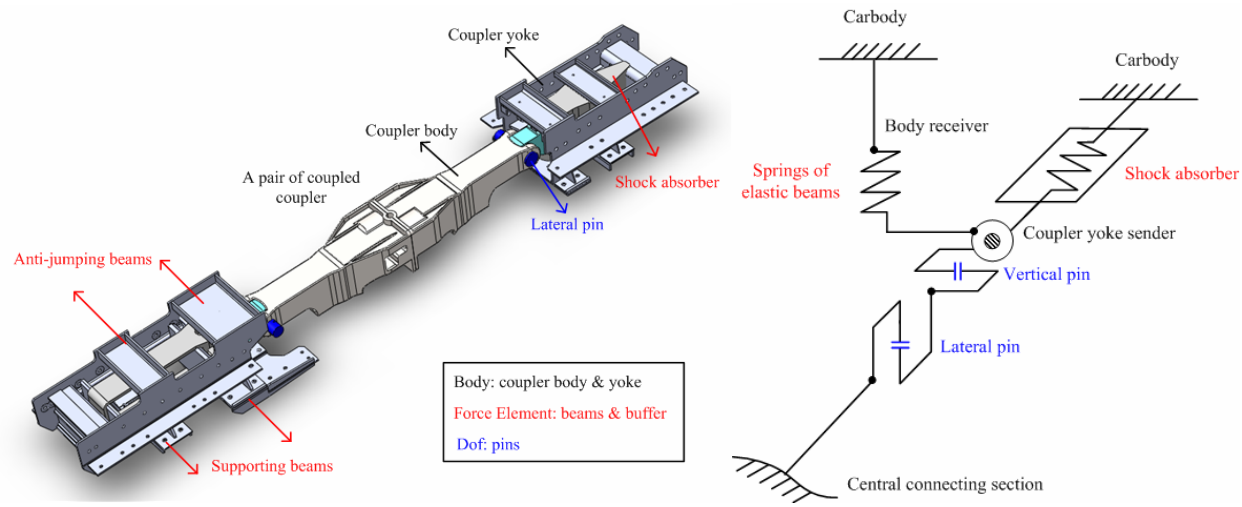

(c) Shibata coupler model

Fig. 5. Dynamic model of train and coupler system.

where M, C, K are the mass, damping and stiffness matrix of the train model respectively, q is state of the train system, $f(\ddot{q},\dot{q},q,t)$ is the nonlinear force elements; D is the distribution matrix of braking torques or forces, and e is the vector of braking torques or forces.

The assisting train in the front is equipped with Shibata couplers while the disabled train with Type 10 coupler. The dynamic model of the coupler system is built based on actual kinetic relations and boundary constraints [19]. Fig. 5(c) shows the Shibata coupler model. For the Shibata coupler, the rotations of the coupler body with respect to the rotational pins are allowable and the relative movements between two coupled couplers in all directions are locked. In normal conditions, the coupler yoke is constrained by the supporting beams and the anti-jumping beams. Thus, in the condition of large vertical force components, the rotation with respect to horizontal axis and the relative movement in vertical and longitudinal directions between the yoke and carbody are free. The boundary constraints of the beams are simulated by vertical springs. The shock absorber is simulated as a longitudinal spring. For

Table 2. Summary of degrees of freedom.

DoFs	Longitudinal	Lateral	Vertical	Roll	Pitch	Yaw
Carbody	v	v	v	v	v	v
Bogie frame	v	v	v	v	v	v
Wheelset	v	v	v	v	v	v
Axlebox					v	
Shibata coupler body					v	v
Shibata coupler yoke	v		v		v	
Type 10 coupler					v	v
Dummy body	v					

the type 10 coupler, the coupler is simplified as a rigid body with only longitudinal DOF. In the central section of the coupled train, an initial pitch angle is considered to simulate the installing height difference between the Shibata coupler and type 10 coupler. The summary of the couplers DOFs is also listed in Table 2.

The look-up table approach is utilized to model the nonlinear hysteresis characteristic of draft gear [20]. The hysteresis characteristic of draft gear means the dissimilarity between its loading and unloading curves. The envelop area between the loading and unloading curves indicates the energy that is absorbed within an operating cycle. The nonlinear characteristics are defined as input functions. The force is given as function of the relative displacement. For a hysteresis model, the upper envelope for positive relative velocities (loading) and the lower envelope for negative relative velocities (unloading) have to be defined. Fig. 6 gives the nonlinear hysteresis characteristic of two types of draft gears according to the drop hammer test. The hysteresis force of the draft gear is defined as:

$$f_{hys} = \left| f_l(x) - f_u(x) \right| . \tag{2}$$

The hysteresis force always acts in the opposite direction of the relative velocity and a sign function is then introduced. The mathematical model of the draft gear can then be expressed as:

$$F = \begin{cases} f + \mathrm{sgn}(v) f_{hys} & |v| > e_v \\ f + v / e_v \cdot f_{hys} & |v| < e_v \end{cases} \tag{3}$$

where F denotes the force of draft gear, v is the relative velocity, f is impedance characteristic of the draft gear depending on the loading or unloading condition, and f_{sys} is the absolute value of the hysteresis force. A regularization velocity is e_v defined to allow a steady transition from one envelope to the other one.

For the electric multiple units (Emus) with train control system, the braking instructions for each vehicle are synchronous. The illustration of the applied braking forces is shown in Fig. 6. For the full-DOF vehicles, the braking torque is applied to

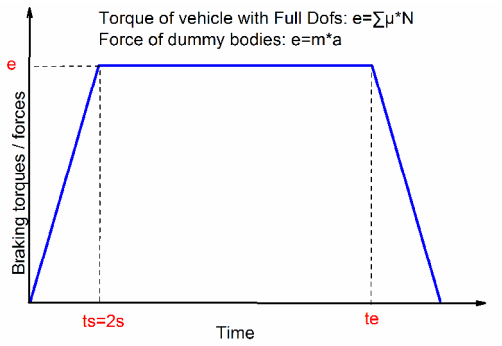

Fig. 6. Illustration of time history of applied braking torques or forces.

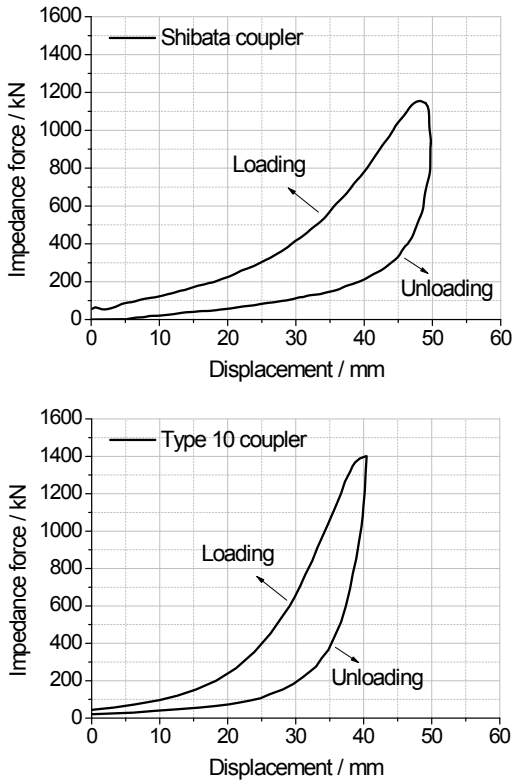

Fig. 7. Nonlinear hysteresis characteristics according to drop hammer test.

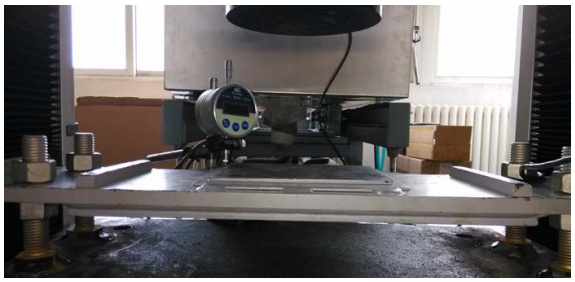

(a) Stiffness test in laboratory

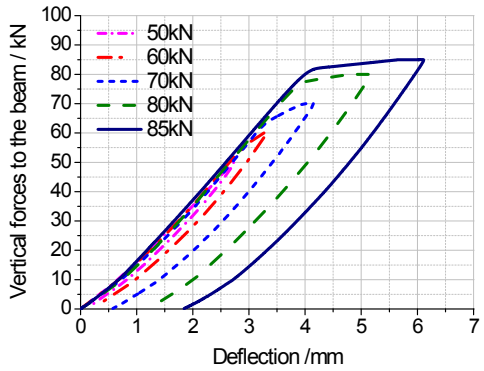

(b) Experimented force-deflection relations

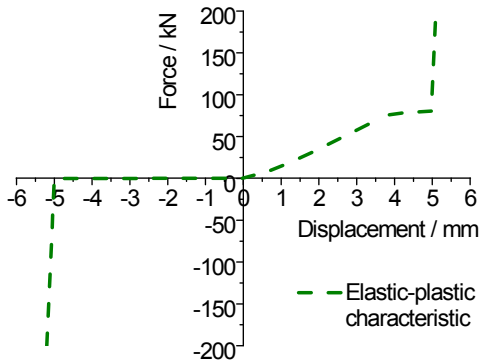

(c) Nonlinear force element in MBS model

Fig. 8. Nonlinear stiffness characteristic of supporting beam of Shibata coupler.

the wheelsets, the amplitude of which is determined by the friction coefficient μ and the normal contact force N of the braking disk. For the dummy vehicles, the braking forces are applied to the center of gravity of the body and the amplitude is calculated by the car body mass m and the equivalent deceleration a. The response time from starting braking to the steady target value is 2.0 sec for the Emus. For the emergency braking, the braking torques is realized by the friction forces of the braking disk and is unrelated to the train speed.

In the Shibata coupler model, the boundary constraints between the coupler yoke and carbody are negligible. It is seen from Fig. 5(c) that the coupler yoke is supported by the beams and limited by the anti-jumping beam. Thus, the stiffness test of the supporting beam was conducted in the laboratory, see Figs. 8(a) and (b), which give the force-deflection relations of the supporting beam subjected to various ranges of the vertical forces. It is indicated that the supporting beam could work in the scale of elastic deformation when the applied force is lower than 70 kN. If the applied force reaches or exceeds 70 kN, slight plastic deformation happens. In actual applications, as slight plastic deformation with 1 or 2 mm of the support beam is acceptable, the limit value of the vertical force for the supporting beam is determined as 80 kN. In the Multi-body system (MBS) dynamic model, the elastic-plastic characteristic of the supporting beam is simplified as a piecewise curve, see Fig. 8(c). The clearance between the coupler yoke and the anti-jumping beam is 5 mm, which is also considered in the model.

3.2 Model verification

In this section, the model verification of case A is conducted by comparing the calculated results with measured results. All the conditions of the simulations are the same to the field tests, including the train configuration, braking deceleration, running speed, etc..

It is seen from Fig. 9(a) that in-train forces are generated due to the application of braking forces. The in-train forces reach the maximum at the start of the application of braking and the low-frequency longitudinal vibration appears. The amplitude of the in-train force decreases gradually under the action of the buffer. The waveform keeps stable till the train stops, then the in-train forces return to normal. The force in the central section is the largest, while that in the disabled train is relatively the smallest. It can be concluded that the calculated in-train forces show good coincidence with the measured results. Fig. 9(b) gives the comparison of the longitudinal decelerations of the vehicles. The waveform of the decelerations is synchronous to the in-train forces. The peak values of the calculated decelerations are close to the measured results.

The laser transducers are used to obtain the relative displacements of couplers and the suspension deflections. The rotational angles can then be determined by the measured displacements and geometry positions. The wheel unloading ratio is calculated by using the indirect wheel-rail force measuring method [21], on the basis of which the wheel-rail vertical forces at two sides of the wheelset can be inversely identified. Fig. 10 gives the comparison of the calculated pitch angles and wheel unloading ratio with the measured results of case A. The relative displacements between the couplers and the adjacent carbodies are measured. The pitch angle of the coupler is determined by this displacement and the rotational length to the lateral pin. The relative displacement between the front coupler and the assisting train is opposite to that of the rear coupler and the disabled train. Thus, it is seen from Fig. 10(a) that the pitch angle of the front coupler is reverse to the rear one. The calculations of the pitch angles of the couplers have good agreement with the measurements. Fig. 10(b) gives the comparison of the pitch angles of the carbodies. It shows that the pitch angle of the assisting train is slightly larger than

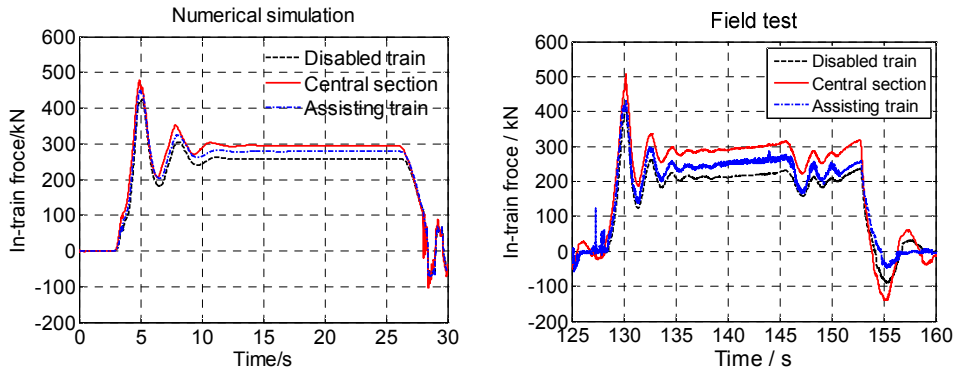

(a) In-train forces

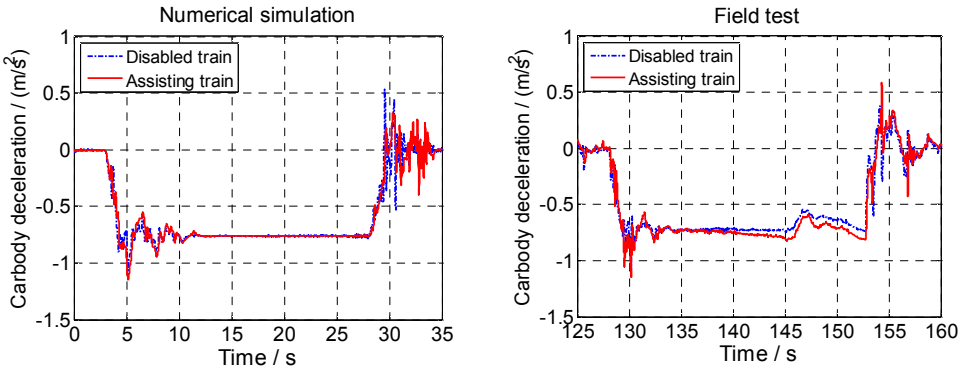

(b) Carbody decelerations

Fig. 9. Comparison of numerical simulations with tested results for case A.

that of the disabled train. The simulated pitch angles of the bodies have good coincidence with the measured results. In general, the coupler angling and the carbody pitching behaviour are well reproduced by numerical simulations. Fig. 10(c) gives the comparison of the wheel unloading ratio, which is defined as the ratio of the unloading force and the nominal wheel-rail force. Therefore, the positive wheel unloading ratio means that the wheelset is unloading. The wheel unloading ratio of the wheelsets close to the central section is measured. It indicates that the wheel in the rear of the assisting train is unloading, while the front of the disabled train is loaded. The simulated wheel unloading ratio is coincident with the measurements.

4. Safety assessment

According to the field test of the 8-8 train configuration (Case A), although the braking induced impacts occurred, the train and coupler systems were not damaged. However, the in-train interference and local structural damages were found in the test of 16-16 train to train rescue (Case B). In this section, the dynamic simulations and safety assessment for the long coupled rescue train, especially for 16-16 train to train rescue scenario, are analysed. Two cases of the train to train rescue scenarios are studied. For train configuration 1, the assisting train in the front is equipped with Shibata couplers while the disabled train in the rear with type 10 couplers. The train configuration 2 is opposite to the train configuration 1. The deceleration of the emergency braking is 1.395 and 0.923 m/s^2 for train configuration 1 and 2, respectively. The running speed of the coupled train is 80 km/h before the application of braking forces.

Fig. 11 gives the simulated time history of the in-train forces and pitch angles. In both cases, the largest in-train force occurs in the central section and the force in the adjacent section of the disabled train is relatively the smallest. The in-train forces of the train configuration 1 are larger than that of the train configuration 2. The generated pitch angles of the three sections with Shibata couplers are shown in Fig. 11(b). Herein, Sec. 1 is just the central connecting section and Secs. 2, 3 are the adjacent sections equipped with Shibata couplers. Similarly, it is seen that the pitch angles of couplers and bodies of the train configuration 1 are larger than that of the train configuration 2. The vertical components of the in-train forces can lead to the vertical angling of the carbody, see Fig. 11(c). The rotation of the carbody is constrained by the air springs. The direction of carbody pitch is opposite to the coupler pitch.

As has been mentioned above, the compressing in-train forces combined with coupler pitch angles can produce vertical force components, which affects the running safeties. According to the testing and numerical investigations, the following safety indices for the train to train rescue scenarios are

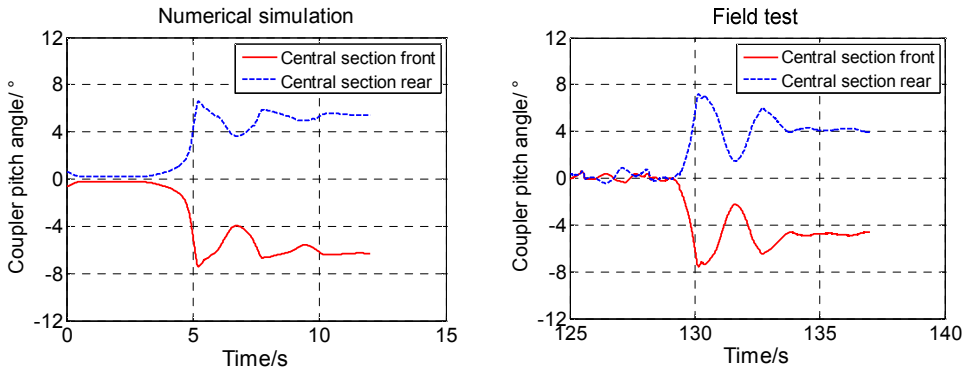

(a) Coupler pitch angle

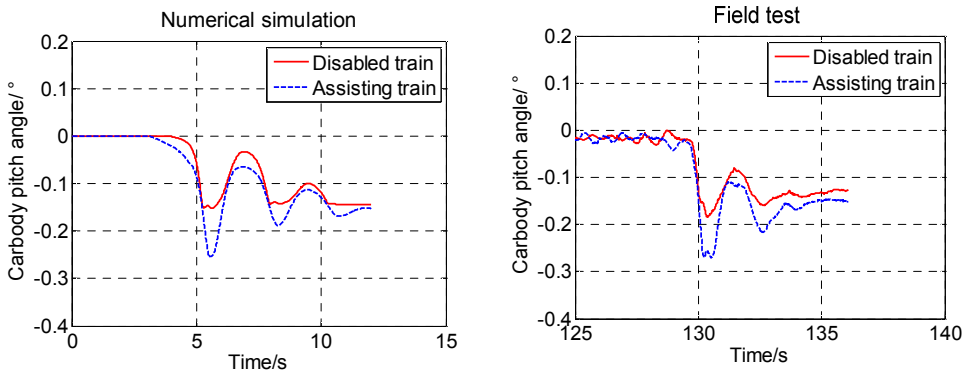

(b) Carbody pitch angle

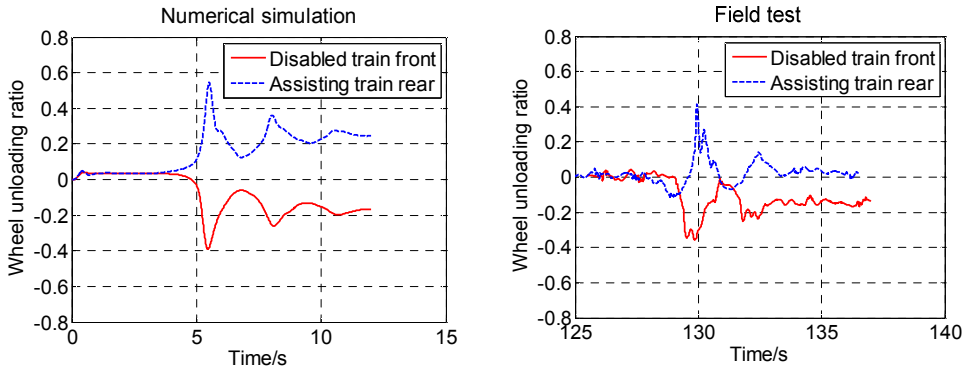

(c) Wheel unloading ratio

Fig. 10. Model verifications for case A.

formulated：

(i) Relative vertical displacement of adjacent carbodies;

(ii) Subjected forces of the supporting beam;

(iii) Wheel unloading ratio.

In order to avoid the interference between the adjacent carbodies, the relative vertical displacement between the adjacent carbodies should be limited. Since there do not exist in-train connections in the central connecting section of two coupled trains, this criteria is only applicable to other connecting sections. The interference between the carbodies equipped with type 10 couplers is not found in the train to train rescue test. Thus, the interference between the carbodies equipped with Shibata couplers is mainly focused. Actually, the relative vertical displacement should be lowered to avoid in-train interference, especially for the in-train dampers. The allowable relative vertical displacement is determined by the clearance between the in-train damper and the carbody frame. The designed value of the clearance between the upper side of in-train damper and the carbody frame is 60 mm, while that in the bottom side is 35 mm. In all, the allowable relative vertical displacement is 95 mm. Besides, in order to avoid structural damages for the train to train rescue scenario during braking, the subjected vertical force of the supporting beam should be limited. According to the stiffness test of the supporting beam,

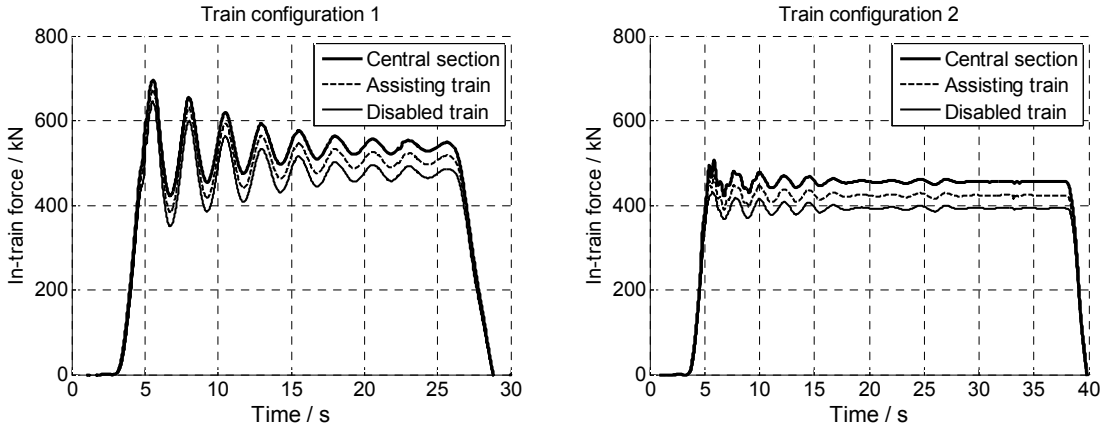

(a) In-train forces

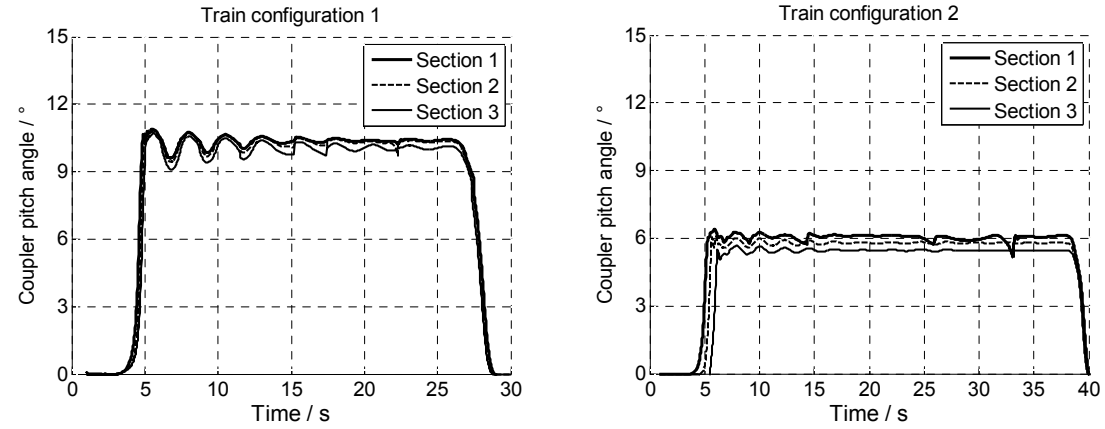

(b) Coupler pitch angle

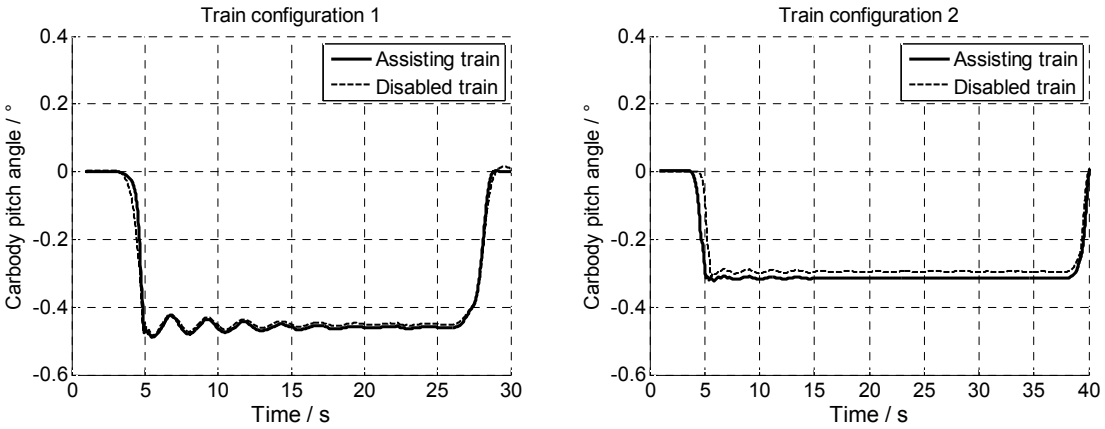

(c) Carbody pitch angle

Fig. 11. Braking induced impacts for two train configurations of case B.

the limit value of the vertical force for the supporting beam is 80 kN when slight plastic deformation of the beam is allowable. The wheel unloading ratio is also used to assess the safety risk of the wheel lift off. According to the GB5599-85 standards [22], the limit value for the wheel unloading ratio is 0.65.

The running safeties of the two train configurations are then evaluated. The safety indices, including the relative displacement of carbodies, vertical force of supporting beam, wheel unloading ratio, are shown in Fig. 12. The vertical relative displacement is generated as a result of the pitch motion of the carbodies. It is seen from Fig. 12(a) that the displacements of the train configuration 1 are larger than that of the train configuration 2. In the case of the train configuration 1, the verti-

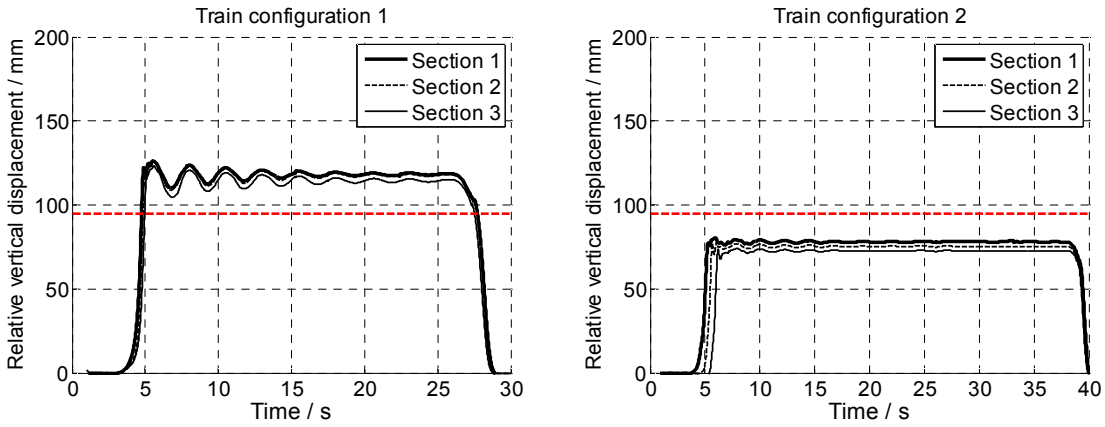

(a) Relative vertical displacements of carbodies

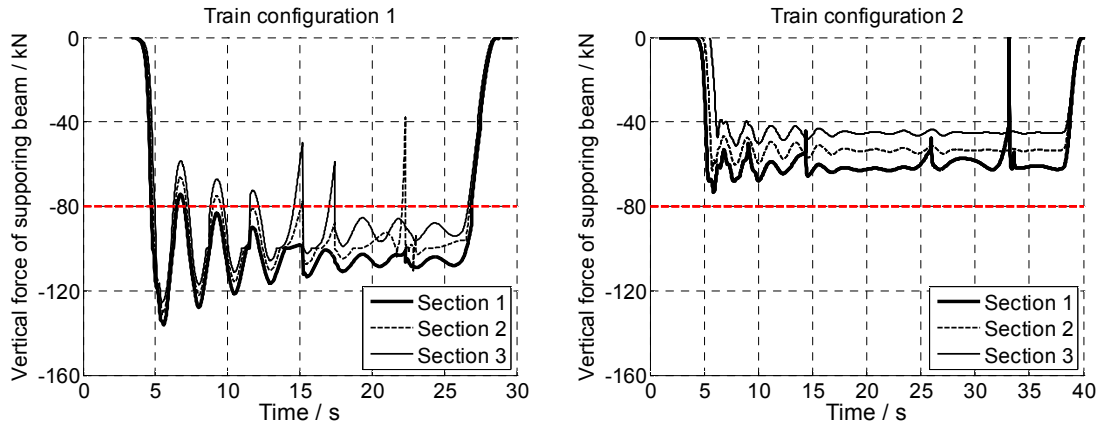

(b) Vertical forces of supporting beams

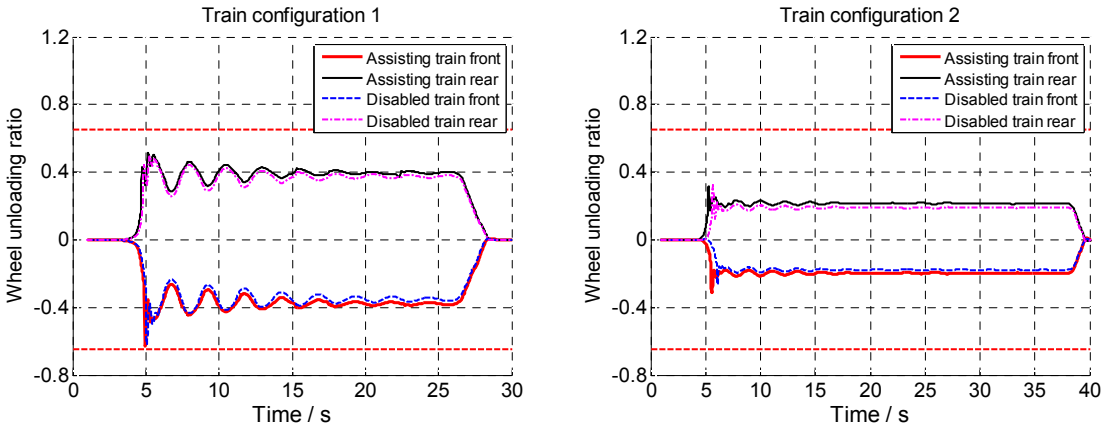

(c) Wheel unloading ratio

Fig. 12. Safety assessments for two train configurations of case B.

cal relative displacements in Secs. 2 and 3 both exceed the limit value, which is coincident with the test phenomenon. Similarly, Sec. 1 is just the central connecting section and Secs. 2, 3 are the adjacent sections equipped with Shibata couplers. For the train configuration 2, the relative displacements are lower than the limit value. The combined in-train forces and coupler angles produce vertical force components. Fig. 12(b) gives the subjected vertical forces of the supporting beams. The forces of the train configuration 1 are larger than that of the train configuration 2. For the train configuration 1, the subjected vertical forces in the three sections all exceed the limit. The subjected vertical forces of the train configuration 2 are lower than the allowable limit. Fig. 12(c) gives the wheel unloading ratio on different wheels. Similarly, the positive

wheel unloading ratio means that the wheelset is unloading. It indicates that the wheels in the rear bogies of both the assisting train and the disabled train are unloading, while the front wheels are loading. The wheel unloading ratio of the train configuration 1 is larger. For train configurations 1, the unloading ratio is quite large, but does not exceed the limit value 0.65. In general, the train to train rescue scenarios are at high risk of causing safety relevant problems. The train configuration 1 is not advised to be used in the actual train to train rescue, while the train configuration 2 is allowable to conduct the train to train rescue.

5. Coupler anti-jackknifing mechanism

5.1 Geometric analysis

In this section, the quasi-static force analysis and anti-jackknifing mechanism of the carbody and coupler system are studied. Due to the application of braking forces, compressing in-train forces are produced. In this paper, it is assumed that only vertical jackknifing of the coupler occurs. The geometry and force variables are show in Fig. 13. Some assumptions are made in the derivation process:

(1) In the quasi-static situation, the center of yoke rotation is assumed to be located in the middle of the yoke. In the dynamic situation, the center of yoke rotation is not defined but is determined by actual boundary constraints.

(2) Similarly, the values of pitch angles for different couplers are assumed to be same in the quasi-static equations because the nonlinear force-displacement relations are not fully considered. Instead, the clearance is adopted in the equations. From the view point the dynamics, the pitch angles for different couplers are close but still have tiny difference, see Fig. 11. This is due to that the pitch angle due to clearance is the same, while that caused by the nonlinear deformation of the supporting beam is different. This is also the difference between the quasi-static equations and dynamic calculations.

(3) In the braking condition, the draft gear will be compressed and the distance will become short. Thus, the value parameter l2 should be smaller. However, the compression value (0.04 m) is quite small and can be ignored if compared with the distance (25.7 m) between pins at two ends of the carbody.

(4) The direction of the force applied to the carbody is directly along the coupler. But the coupler gravity is not considered in the derivation process and is thought to be has no influence on the coupler forces. In dynamic situations, this force may also be affected by the inertial force of the coupler itself but cannot be considered in the quasi-static situation.

(5) The coordinate system in this paper is connected with gravity center of the carbody. All the geometry and force analysis are carried out according to this center.

The pitch angle of the carbody γ_1 is determined by the ratio of the sum of suspension deflections to the bogie center distance.

$$\gamma_1 = \arcsin\left(\frac{-d_{s1} + d_{s2} - d_{p1} + d_{p2}}{l_1}\right) \tag{4}$$

where d_{s1} is the compressed deflection of the air spring in bogie 1 and d_{s2} is the tensional deflection of the air spring in bogie 2, d_{p1} is the compressed deflection of the primary spring in bogie1 and d_{p2} is the tensional deflection of the primary spring in bogie 2, and l_1 represents the bogie center distance. The vertical distance between adjacent coupler pins is written as below:

$$h_1 = \sin\gamma_1 \cdot l_2 \tag{5}$$

where l_2 indicates the distance between coupler rotational pins at two ends of the carbody.

Besides, the vertical rotation of the coupler yoke also occurs. As the yoke is supported by two pieces of beams, the center of them is assumed to be the rotational center. The rotation of the yoke is limited by the boundary constraint and the allowable pitch angle of the yoke is expressed as:

$$\gamma_2 = \arcsin\left(\frac{d_{z1} + d_{z2}}{l_3}\right) \tag{6}$$

where d_{z1} is the clearance between the coupler yoke and the supporting beam, d_{z2} is the clearance between the coupler yoke and the anti-jumping beam, and l_3 is the distance from the front supporting beam to the rear beam. The vertical displacement of the pin caused by the pitch motion of the yoke is written as:

$$h_2 = \sin\gamma_2 \cdot (l_3/2 + l_4) \tag{7}$$

where l_4 denotes the distance between the pin and front supporting beam. The relative vertical displacement between lateral pin of couplers includes the displacement due to the carbody pitch as well as that due to the yoke pitch. The overall pitch angle of the coupler can then be determined as below:

$$\gamma_3 = \arcsin\left(\frac{h_1 + 2h_2}{l_5}\right) \tag{8}$$

where l_5 is the length of coupler body.

5.2 Anti-jackknifing mechanism

The anti-jackknifing mechanism of coupler and carbody is then studied. The carbody is subjected to compressing in-train forces F_1 and F_2 from couplers. With respect to the gravity center of the carbody, the pitch moment due to the in-train forces is written as below:

$$\begin{aligned} M_p = {} & (F_{zc1} + F_{zc2}) \cdot (l_1/2 + l_6) + F_{xc1} \cdot (h_3 + h_1/2 + h_2) \\ & - F_{xc2}(h_3 - h_1/2 - h_2) \end{aligned} \tag{9}$$

Table 3. Basic parameters of the train and coupler system.

Parameters	Symbols	Value	Unit
Maximum compressed deflection of air spring	d_{s1}	-43	mm
Maximum tensional deflection of air spring	d_{s2}	70	mm
Vertical stiffness of single air spring	k_{sz}	0.3	MN/m
Vertical stiffness of single primary spring	k_{pz}	0.7	MN/m
Clearance between the yoke and front supporting beam	d_{z1}	2.7	mm
Clearance between the yoke and anti-jumping beam	d_{z2}	5	mm
Bogie center distance	l_1	17.5	m
Distance between pins at two ends of the carbody	l_2	25.7	m
Distance from front the supporting beam to the rear	l_3	0.1716	m
Distance between the pin and front supporting beam	l_4	0.6432	m
Length of coupler body	l_5	1.6	m
Distance from the pin to bogie center	l_6	2.307	m
Height from carbody gravity center to coupler installing position	h_3	0.52	m
In-train force of coupler 1	F_1	675	kN
In-train force of coupler 2	F_2	700	kN

where F_{zc1} and F_{zc2} are the vertical force component of coupler 1 and 2. F_{xc1} and F_{xc2} are the longitudinal force component of coupler 1 and 2. h_3 is the height from the gravity center of the carbody to the initial installing position of the coupler. The counter-clockwise direction is defined as positive. With the application of braking forces, the vertical force components of the couplers can be calculated as follows:

$$F_{zci} = F_i \cdot \sin\gamma_3,\ F_{zxi} = F_i \cdot \cos\gamma_3\ (i = 1,2)\,. \tag{10}$$

Meanwhile, the anti-pitch moment of the carbody is provided by air springs. The vertical force of bogie 1 decreases; on the contrary, the vertical force of bogie 2 increases. The anti-pitch moment with respect to gravity center of the carbody is:

$$M_s = -(2F_{zs1} - 2F_{zs2}) \cdot l_1 / 2 \tag{11}$$

where, F_{zs1} and F_{zs2} are half of the vertical forces of bogies 1 and 2, respectively. The moment-balanced equation of carbody is then determined by Eqs. (9) and (11).

$$\begin{aligned}&(F_{zc1} + F_{zc2}) \cdot (l_1 / 2 + l_6)\\ &+F_{xc1} \cdot (h_3 + h_1 / 2 + h_2)\\ &= F_{xc2}(h_3 - h_1 / 2 - h_2) + (F_{zs1} - F_{zs2}) \cdot l_1\,.\end{aligned} \tag{12}$$

In the vertical direction, the force-balanced equation is built.

$$F_{zc1} - F_{zc2} - 2F_{zs1} - 2F_{zs2} + G = 0\,. \tag{13}$$

The vertical forces of air springs can then be derived from Eqs. (12) and (13):

$$\begin{aligned}F_{zs1} = {} & F_{zc1}(1 + l_6 / l_1) + F_{zc2} \cdot l_6 / l_1\\ & + F_{xc1}(h_3 + h_1 / 2 + h_2) / 2l_1\\ & - F_{xc2}(h_3 - h_1 / 2 - h_2) / 2l_1 + G / 4\end{aligned} \tag{14}$$

and

$$\begin{aligned}F_{zs2} = {} & F_{zc1}(1 + l_6 / l_1) - F_{zc2} \cdot l_6 / l_1\\ & - F_{xc1}(h_3 + h_1 / 2 + h_2) / 2l_1\\ & + F_{xc2}(h_3 - h_1 / 2 - h_2) / 2l_1 + G / 4\,.\end{aligned} \tag{15}$$

Based on the geometry and force analyses mentioned above, the influence of basic parameters on the pitch angle and unloading forces is studied. The influence of the secondary clearance and bogie center distance on the carbody pitch angle is shown in Fig. 14(a). Herein, the secondary clearance is the sum of the compressed and the tensional clearance of air springs. The carbody pitch angle decreases with the increasing of bogie center distance. The decrease of the secondary clearance is beneficial to lower the carbody pitch angle. The influence of the distance between pins and the length of coupler on the coupler pitch angle is shown in Fig. 14(b). The increase of the length of coupler is beneficial to prevent the coupler pitch. The coupler pitch angle increases with the increasing distance

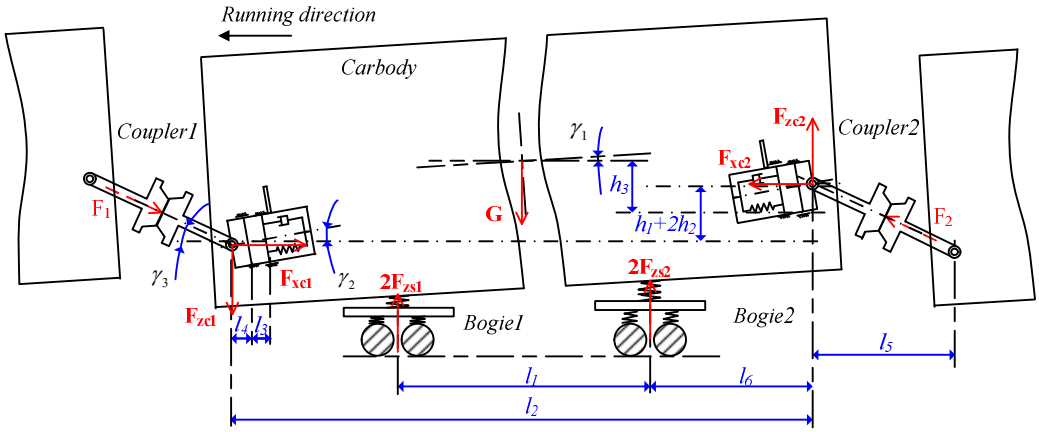

Fig. 13. Geometry and force variables illustration of carbody and couplers.

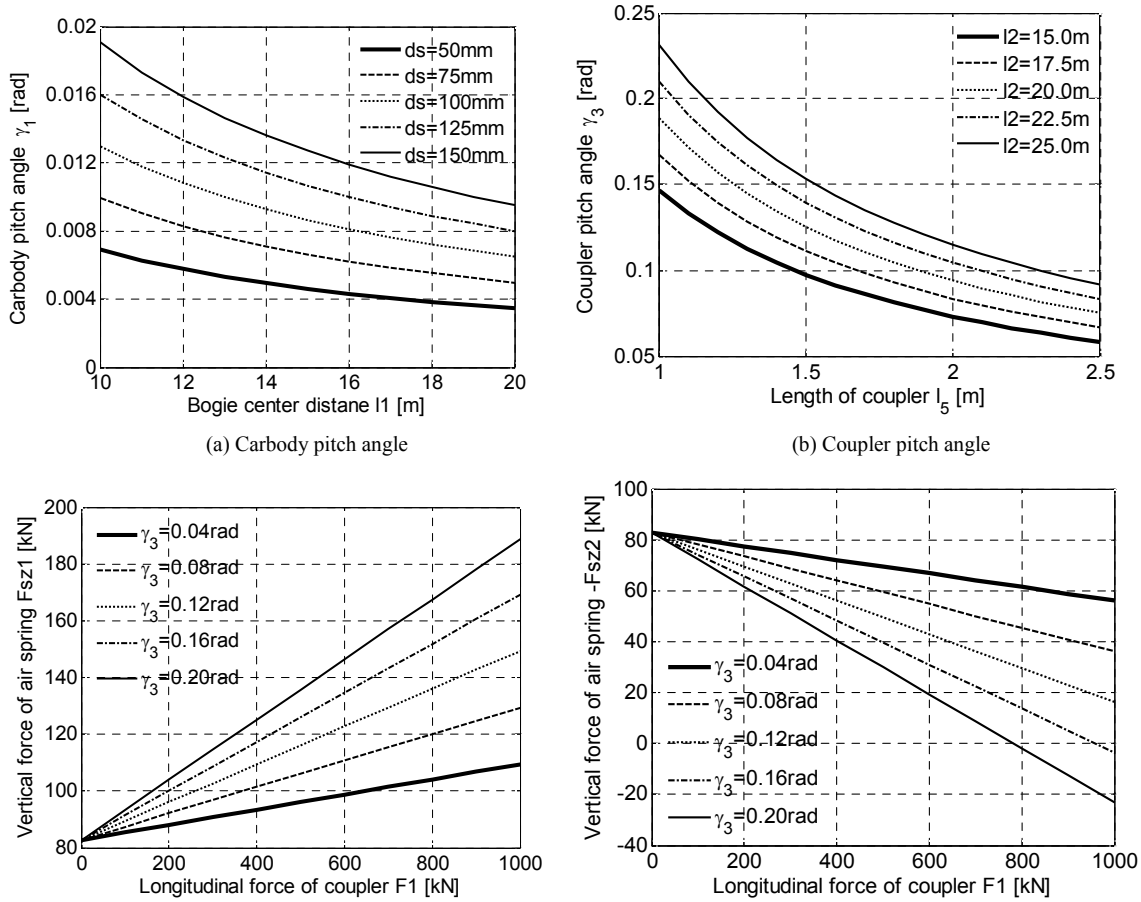

(a) Carbody pitch angle

(b) Coupler pitch angle

(c) Vertical force of air spring 1

(d) Vertical force of air spring 2

Fig. 14. Influence of basic parameters on geometry and force states.

between pins at two ends of the carbody.

The influence of the in-train forces and the coupler pitch angle on the vertical forces of air springs is also studied. In the quasi-static analysis presented in Fig. 13, the air spring is thought to be linear but with limited clearance. The objective is to propose a general description of braking induced in-train problems, including geometry and force analysis. While in the train dynamic model, the air spring is modeled with nonlinear physical model with considering the internal structure, e.g. air pressure & density, pipes length & diameter and additional gas chamber, etc. The modeling of the air spring has been presented in the paper before and is not the key of this paper.

It is seen from Fig. 14(c) that the vertical force of the air spring in bogie 1 increases with the increasing of longitudinal

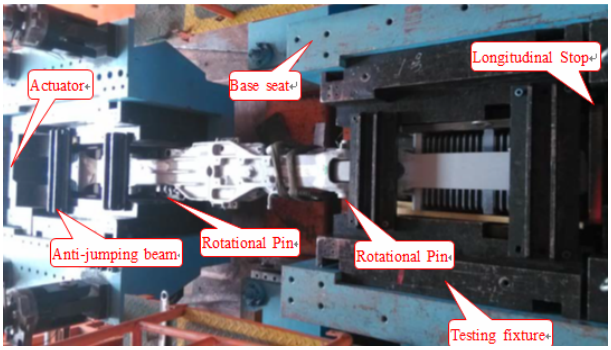

Fig. 15. Illustration of coupler propelling test.

force and coupler pitch angle. The vertical force of the air spring in bogie 2 decreases with the increasing of longitudinal force and coupler pitch angle, see Fig. 14(d). The unloading forces of air springs are produced by the combination of the longitudinal force and the coupler pitch angle.

5.3 Coupler propelling test on test rig

In order to reproduce the coupler jackknifing under longitudinal forces, the coupler propelling test on the test rig was carried out in the laboratory of Sifang Rolling Stock Research Institute, as shown in Fig. 15. The test rig consists of two pairs of base seats and testing fixtures. In order to simulate actual boundaries, the tested coupler is supported by beams under the coupler and limited by anti-jumping beams above the coupler. The longitudinal movement of the coupler is limited by the stop of the testing fixture in the right hand. The actuator in the left side is used to propelling the coupler and the force is applied gradually. The vertical movement of the testing fixture is allowable. Therefore, once the coupler jackknifing happens during the test, the vertical force component could jack up the testing fixture.

The propelling tests were conducted in two cases, one is without initial coupler pitch angle (Case 1) and another is with an initial pitch angle of 0.9° (Case 2). It is known from the test results that the coupler vertical angling behavior appeared with the propelling force increases to 480 kN for case 1. The testing fixture is jacked up by 400 mm due to the vertical component of the longitudinal force, shown in Fig. 16. For test case 2, the critical force is 365 kN when the testing fixture climbed upwards. The coupler with an initial pitch angle is more easy to be unstable than that without initial pitch angle. The coupler system can only keep stability in theoretically straight situations. In the propelling test, the critical situation to instability is that the vertical component reaches the sum of the gravity and the friction force of the testing fixture.

6. Parametric studies and improvement measures

In this section, parametric studies for the train configuration 1 are conducted to find some solutions to lower the braking

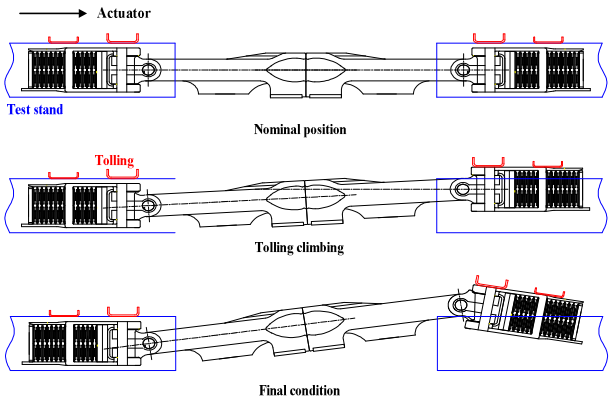

(a) Illustration of coupler longitudinal instability

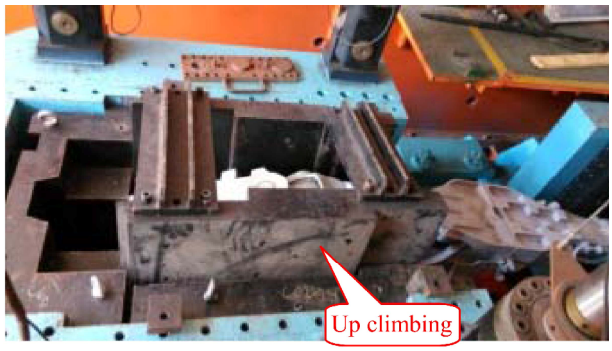

(b) Up-climbing behaviour of testing fixture

Fig. 16. Reproducing of coupler vertical jackknifing on test rig.

induced impacts and relevant safety indices. On one hand, the in-train forces should be decreased; on the other hand, the pitch angle of the coupler should be limited. As the train to train rescue is used for the operating trains, structural modifications are not allowed. Fig. 17 shows the influence of braking levels on the braking induced impacts. The emergency braking level is shorted as Em and the No.7 braking level is denoted as 7 N. The braking decelerations for the Em, 7 N, 6 N and 5 N braking are 1.395, 0.721, 0.627 and 0.533 m/s^2, respectively. The in-train forces and buffer displacements decrease significantly with decreasing decelerations, as a result of which the amplitudes of pitch angles and vertical forces are also reduced. It is concluded that the lower the braking levels or the decelerations, the smaller the braking induced impacts.

Fig. 18 shows the influence of the free rotational angles of couplers on the braking induced impacts. The free rotational angle means the maximum allowable pitch angle with respect to the lateral pin of the coupler. It is reported in literature that the coupler shoulders and the pin shapes can be designed to provide limitation to the rotation of the coupler [10]. Besides, the decrease of secondary clearances can also reduce the free rotational angle of the coupler. Herein, the free rotational angle is virtually set up in the simulations. It is seen that the free rotational angle of the coupler has little influence on the in-train forces and buffer displacements. The increase of the free rotational angle of the coupler is beneficial to reduce the pitch

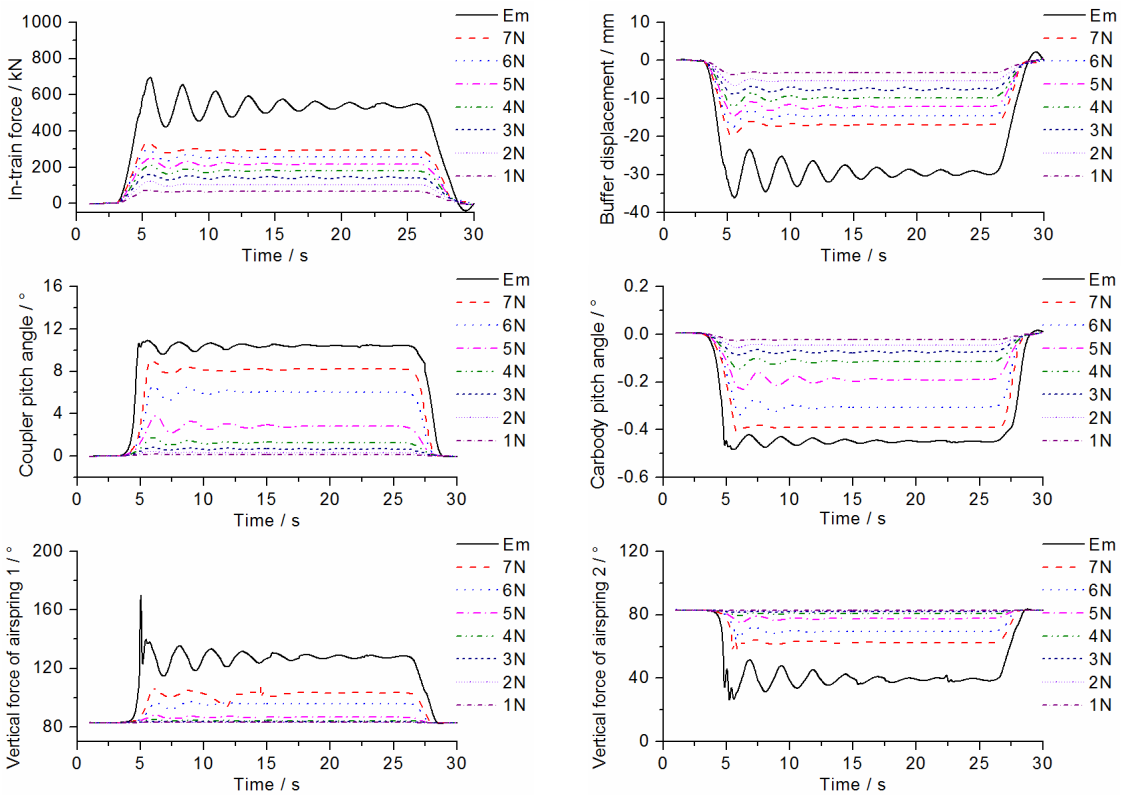

Fig. 17. Influence of braking levels on braking induced impacts.

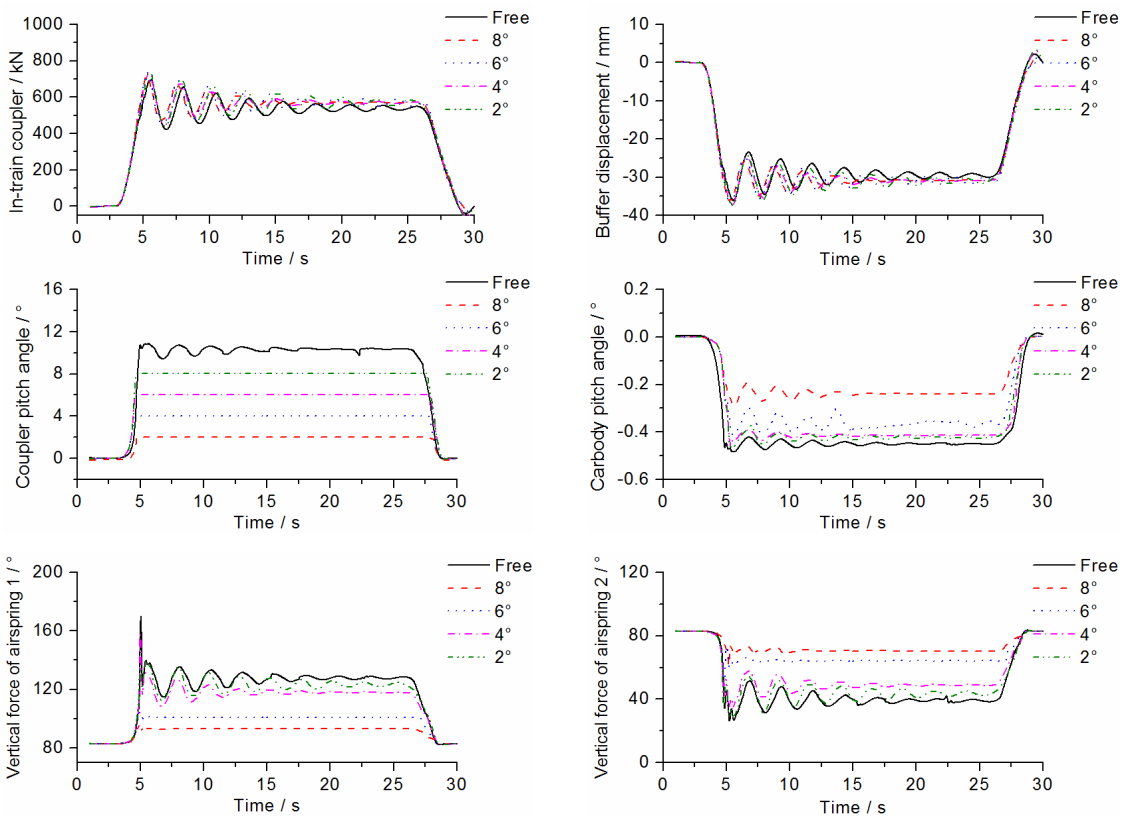

Fig. 18. Influence of free rotational angles on braking induced impacts.

Table 4. Summary of calculated safety indices for different cases.

Parameters				Safety indices		
Train configuration	Train speed km/h	Braking	Free angle of coupler	Vertical force	Relative displacement	Wheel unloading ratio
8-16	80	Em	Free	√	×	√
16-8	80	Em	Free	√	×	√
8-8	80	Em	Free	√	√	√
16-16	60	Em	Free	×	×	×
16-16	80	Em	Free	×	×	√
16-16	120	Em	Free	×	×	√
16-16	80	7N	Free	×	√	×
16-16	80	6N	Free	√	√	√
16-16	80	5N	Free	√	√	√
16-16	80	Em	8°	×	×	√
16-16	80	Em	6°	×	×	√
16-16	80	Em	4°	√	×	√
16-16	80	Em	2°	√	√	√

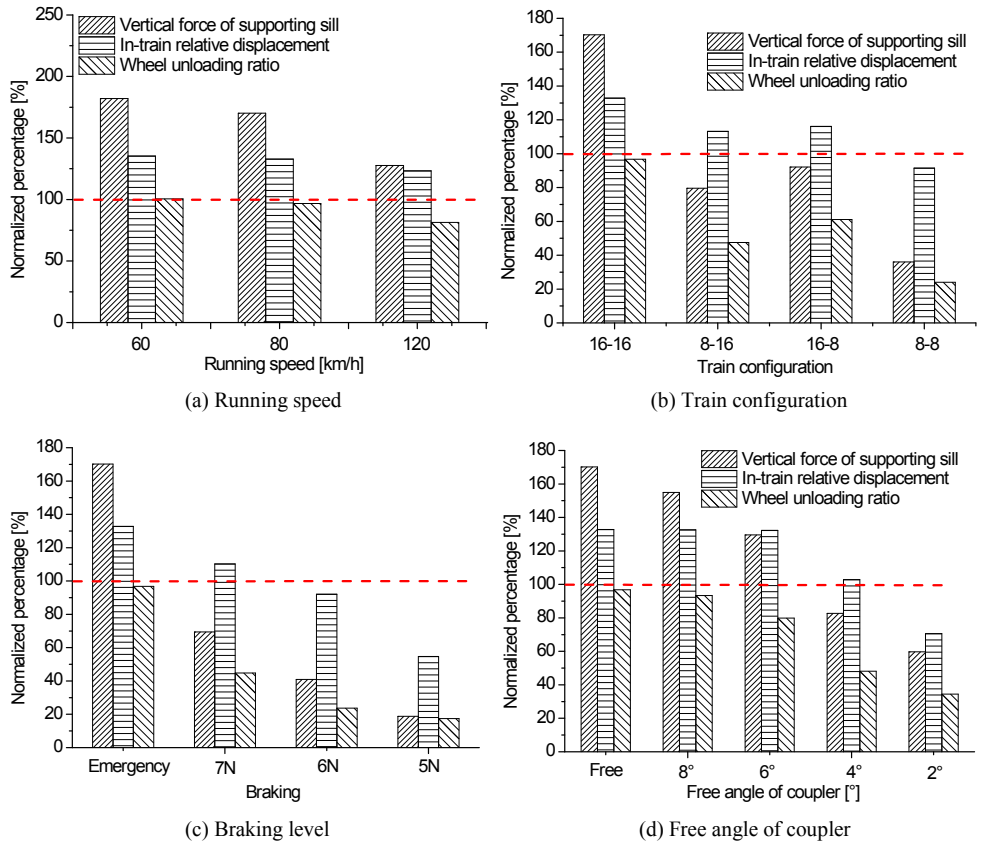

(a) Running speed

(b) Train configuration

(c) Braking level

(d) Free angle of coupler

Fig. 19. Influence of some basic parameters on normalized safety indices.

angles of the coupler and the carbody. Therefore, the amplitude of the vertical forces of air springs decreases with decreasing free rotational angles. It is concluded that the smaller the free rotational angle of the coupler, the smaller the braking induced impacts.

Furthermore, the safety analysis for different parameters is performed. The influences of the running speed, train configuration, braking deceleration and free angles on the safety indices are studied. In order to compare various safety indices, the normalized percentage defined as the ratio of the actual value and the limit value is adopted. Fig. 19(a) gives the influence of the train speed on the normalized indices. For the train con-

figurations 1, the emergency braking under different speeds is applied by the assisting train. According to the braking characteristic, the decelerations of the emergency braking are 1.395, 1.318 and 1.019 m/s^2 for the speed of 60, 80 and 120 km/h, respectively. It is indicated that the safety indices decrease with the increasing speed or the actually decreasing braking deceleration. Fig. 19(b) gives the influence of the train configurations on the normalized indices. The emergency braking is applied by the assisting train at the speed of 80 km/h. The train to train rescue scenario consisting of 16 assisting cars and 16 disabled cars is termed as 16-16 train configuration. Similarly, the 16-8, 8-16 and 8-8 train configurations are also defined. It is seen that the safety indices for the 16-16 train configuration is the largest, while that for the 8-8 train configuration is the lowest. Therefore, the shorter the length of coupled train, the smaller the braking induced impacts. The safety indices of the 16-16, 16-8 and 8-16 exceed the limits meaning that these train configurations are risky in causing safety problems during emergency braking. Fig. 19(c) shows the influence of braking levels on the normalized indices at the speed of 80 km/h. The decelerations are 0.721, 0.627 and 0.533 m/s^2 for the 7 N, 6 N and 5 N braking level, respectively. It is found that the decrease of the braking deceleration is beneficial to lower braking induced impacts. Fig. 19(d) shows the influence of the coupler free angles on the normalized indices. The emergency braking is applied by the assisting train at the speed of 80 km/h. It is known that the safety indices decrease with the increasing free angle of the coupler. In actual applications, some structural modifications should be considered in designs to provide a limitation to the rotation of the coupler. In numerical simulations, it shows that a limitation of the free pitch angle of a coupler is beneficial to decrease the braking induced impact. In actual application for tight lock couplers used in high speed passenger cars, the coupler rotations are free. In heavy-haul trains or locomotives, some limitations been used in engineering. For instance, the friction in the coupler system can decrease to coupler angle (see Ref. [10]). Besides, a specially designed rope can be installed to avoid two large coupler angles.

The summary of calculated safety indices for different cases is listed in Table 4. It can be concluded that the decrease of the braking deceleration is beneficial to reduce the in-train force and the limitation of the free pitch angle of the coupler can decrease the pitch angles of the coupler and the carbody. From the view point of the application of the train to train rescue, the 16-16, 16-8 and 8-16 train configurations are at risk of causing the interference of in-train connections and structural damages. In order to prevent these safety relevant problems for the 16-16 train to train rescue scenario (train configuration 1), the braking level should be lower than 6 N or the free pitch angle of the coupler limited within 2°.

7. Conclusions

The studies on the in-train stability and safety assessment for train to train rescue scenarios during braking are conducted in this paper and it can be concluded as follows:

(1) The investigation of the coupler jackknifing behaviour for the train to train rescues is carried out. The compressing in-train force due to braking has an adverse effect on the longitudinal stability of either the train or the coupler system. The combination of the in-train force and the coupler pitch angle generates a vertical force component, which may further lead to the carbody pitching and wheel unloading.

(2) The dynamic models of the train and coupler system are developed. The model verification for the train to train rescue scenario is conducted and the calculated results show good agreement with the measured ones. The braking induced impacts, including the in-train force, the coupler pitch angle and the carbody pitch angle, are reproduced. The in-train force if combined with the coupler pitch angle can produce vertical force component which affects the running safety of the coupled train.

(3) The quasi-static force analysis and measures preventing the potential development of the jackknifing are studied. It is known that the increase of the bogie center distance or the increase of secondary clearance can reduce the carbody pitch angle. The increase of the coupler length or the decrease of the distance between pins is beneficial to decrease the coupler pitch angle. The anti-pitch moments against the pitch moment caused by the in-train forces are provided by the vertical forces of the air springs.

(4) It is seen from parametric studies that the in-train force can be reduced by decreasing the braking deceleration, while the pitch angle can be decreased by the limitation of the free rotational angle of the coupler. In order to prevent the safety relevant problems for the 16-16 train to train rescue scenario, the braking level should be lower than 6 N or the free pitch angle of the coupler limited within 2°.

In this paper, it is concluded that the so called in-train stability problem occurs in the braking condition of railway vehicles, which refers to the jackknifing behavior. The combination of in-train force and coupler pitch has significant effect on the system response and running safety. Two ways including decreasing in-train force or limiting coupler rotations can prevent the potential risk due to in-train stability problem.

Acknowledgment

This work was supported by the National Natural Science Foundation of China (Grant No.U1334206), Science & Technology Development Project of China Railway Corporation (Grant No.2014J012-C) & the Fundamental Research Funds for the Central Universities (No.2682014CX029). Acknowledgment is also made to Sifang Rolling Stock Research Institute for supporting the tests of this research.

References

[1] R.C. Li, Unified design for draught-gear for electric multiple

unit, *Urban Mass Transit*, 16 (8) (2013) 64-69.
[2] K. Chen and Q. Qian, Test and research on mutual rescue between multiple units of different types, *Rolling Stock*, 52 (5) (2014) 1-5.
[3] D. Chen, Derailment risk due to coupler jack-knifing under longitudinal buff force, *Proceedings of the Institution of Mechanical Engineers, Part F: Journal of Rail and Rapid Transit*, 224 (5) (2010) 483-490.
[4] G. M. Magee, W. M. Keller and R. Ferguson, *Jackknifing of diesel electric locomotives report of the joint committee on relation between track and equipment*, Report No.10838, Association of American Railroads (AAR), Washington DC, USA (1955).
[5] M. El-Sibale, Recent advancements in buff and draft testing techniques, *Proceedings of 1993 IEEE/ASME Joint Conference*, ASME, NewYork, USA (1993) 115-119.
[6] M. McClanachan et al., An investigation of the effect of bogie and wagon pitch associated with longitudinal train dynamics, *Proceedings of the 16th IAVSD Symposium*, Pretoria, South Africa (1999).
[7] S. Wagner, *Derailment risk assessment*, James Goldston Faculty of Engineering and Physical Systems, Central Queensland University (2004).
[8] C. Cole and Y. Q. Sun, Simulated comparisons of wagon coupler systems in heavy haul trains, *Proceedings of the Institution of Mechanical Engineers, Part F: Journal of Rail and Rapid Transit*, 220 (3) (2006) 247-256.
[9] C. Cole et al., Wagon instability in long trains, *Vehicle System Dynamics*, 50 (1) (2012) 303-317.
[10] Q. Wu et al., Coupler jackknifing and derailments of locomotives on tangent track, *Vehicle System Dynamics*, 51 (11) (2013) 1784-1800.
[11] Z. Q. Xu et al., Coupler rotation behaviour and its effect on heavy haul trains, *Vehicle System Dynamics*, 51 (12) (2013) 1818-1838.
[12] S. H. Luo, Q Feng and J. J. Yang, Research on dynamics of the HXD2 heavy locomotive bearing longitudinal compressive strength, *Railway Locomotive & Car*, 28 (2008) 145-149.
[13] W. H. Ma, S. H. Luo and R. Song, Coupler dynamic performance analysis of heavy haul locomotives, *Vehicle System Dynamics*, 50 (9) (2012) 1435-1452.
[14] M. El-Sibaie and T. T. Center, *Dynamic buff and draft testing techniques*, Association of American Railroads Transportation Test Center (AAR/TTC) (1992).
[15] AS 7509.2, *Railway rolling stock- dynamic behaviour -part 2: Freight Rolling Stock*, Australia and Rail Industry Safety & Standards Board, Canberra, Australia (2009).
[16] BS EN 14363, *Railway applications-testing for the acceptance of running characteristics of railway vehicles- testing of running behavior and stationary tests*, CEN, Brussels (2005).
[17] UIC 530-2, *Wagons - Running Safety*, 7th ed., International Union of Railways, Paris (2011).
[18] TSI 2008/232/CE, Concerning a technical specification for interoperability relating to the 'rolling stock' sub-system of the trans-European high-speed rail system, *Official Journal of the European Union* (2008).
[19] N. Nakano and Y. Terumichi, Numerical analysis for coupled train considering 3D wheel/rail contact geometry, *Journal of Mechanical Science and Technology*, 29 (7) (2015) 2677-2683.
[20] Q. Wu et al., Dynamics simulation models of coupler systems for freight locomotive, *Journal of Traffic and Transportation Engineering*, 12 (3) (2012) 37-43.
[21] L. Wei et al., Indirect method for wheel-rail force measurement and derailment evaluation, *Vehicle System Dynamics*, 52 (12) (2014) 1622-1641.
[22] GB 5599-85, *Railway vehicles-specification for evaluation the dynamic performance and accreditation test*, 1st ed., National Bureau of Standard, Beijing, China (1985).
[23] H. Esfandiar and M. H. Korayem, Accurate nonlinear modeling for flexible manipulators using mixed finite element formulation in order to obtain maximum allowable load, *Journal of Mechanical Science and Technology*, 29 (9) (2015) 3971-3982.
[24] X. Xu, S. Dong, J. Luo and T. Luo, The nonlinear effects of flexible pins on wind turbine gearboxes, *Journal of Mechanical Science and Technology*, 29 (8) (2015) 3077-3082.
[25] J. S. Koo and H. S. Oh, A new derailment coefficient considering dynamic and geometrical effects of a single wheelset, *Journal of Mechanical Science and Technology*, 28 (9) (2014) 3483-3498.
[26] C. J. Park and G. Gschwendtner, Braking performance analysis of an escalator system using multibody dynamics simulation technology, *Journal of Mechanical Science and Technology*, 29 (7) (2015) 2645-2651.

Lai Wei received his doctor degree in vehicle operation engineering from Southwest Jiaotong University in 2015. He is interested in the areas of numerical calculation, laboratory experiments and field testing for railway vehicles.